Reversible Bending Fatigue Testing on Zry-4 Surrogate Rods – 14503

Jy-An Wang, Hong Wang, Bruce Bevard, and Robert Howard
Oak Ridge National Laboratory

ASTRACT

Testing high-burnup spent nuclear fuel (SNF) presents many challenges in areas such as specimen preparation, specimen installation, mechanical loading, load control, measurements, data acquisition, and specimen disposal because these tasks are complicated by the radioactivity of the test specimens. Research and comparison studies conducted at Oak Ridge National Laboratory (ORNL) resulted in a new concept in 2010 for a U-frame testing setup on which to perform hot-cell reversible bending fatigue testing. Subsequently, three-dimensional finite element analysis and engineering design of components was completed. In 2013 the ORNL team finalized the upgrade of the U-frame testing setup and the integration of the U-frame setup into a Bose dual linear motor test bench to develop a cyclic integrated reversible-bending fatigue tester (CIRFT). A final check was conducted on the CIRFT test system in August 2013, and the CIRFT was installed in the hot cell in September 2013 to evaluate both the static and dynamic mechanical response of SNF rods under simulated loads.

The fatigue responses of Zircaloy-4 (Zry-4) cladding, including understanding the role of pellet–pellet and pellet–clad interactions are critical to characterizing SNF vibration integrity, but such data are not available due to the unavailability of an effective testing system. While the deployment of the CIRFT test system in a hot cell will provide the opportunity to generate this data, the use of surrogate rod testing has proven quite effective in identifying the underlying deformation mechanism of a cladding and fuel composite rod under an equivalent loading condition. This paper presents the experimental results of using surrogate rods under CIRFT reversible cyclic loading. Specifically, monotonic and cyclic bending tests were conducted on surrogate rods made of a Zry-4 tube and alumina pellet inserts, both with and without an epoxy bond.

INTRODUCTION

Transportation packages for SNF must meet safety requirements under normal and accident conditions as specified by federal regulations. During transportation, SNF may experience unique conditions and challenges to cladding integrity due to the vibrational loading encountered during road or rail shipment. ORNL has been developing testing capabilities that can be used to improve our understanding of the impacts of vibration loading on SNF integrity, especially for high burn-up SNF in normal transportation operation conditions. This information can be used to meet nuclear industry and U.S. Nuclear Regulatory Commission needs in the area of safety of SNF transportation operations.

The major considerations during testing the high-burnup SNF rods include:

- High-burnup SNF rods have a composite structure with multiscale discontinuities.
- Pellet–pellet interfaces and normal stresses parallel to the longitudinal axis of the SNF rod maybe a significant rod failure mechanism under cyclic bend loading.
- Shearing-dominant fractures and contact-induced damage in a conventional four- or three-point bending setup readily induce failures away from the target locations.
- A free-fixed (FRFXD) type of boundary condition is required at the specimen grip ends to ensure the rod specimen can move freely in the axial direction under bend loading, which significantly increases the degree of difficulty in U-bend apparatus design.

- equipment of the testing setup in a hot-cell environment imposes strict constraints on the test design.

An extensive literature survey revealed a variety of existing bending fatigue testing methods, including cantilever beam bending, three- or four-point bending, pure bending, as well as systems taking into account environmental-factor considerations, particularly temperature. However, these conventional systems do not meet the challenges and constraints uniquely related to vibration integrity studies on SNF rods.

Research and comparison studies conducted in 2010 at ORNL resulted in a new concept for a U-frame testing setup on which to perform hot-cell reversible bending fatigue testing.[1] Subsequently, three-dimensional finite element analysis and engineering design of the system components were completed. The first prototype of the U-frame was assembled and mounted to an MTS servo-hydraulic testing machine in June 2011.[2] Many issues with the reversible cyclic bending were evaluated during calibration and testing even though the proof-of-concept had been demonstrated. These issues covered a variety of areas, such as installation of the rod specimen into the bending device, measurement of rod bending, selection of the driving system for the hot cell, etc. The technical challenges included developing a proper specimen holder, effective implementation of the FRFXD boundary condition, and mitigation of the components' weight on sample bending deformation.[3] From 2012 to 2013 the ORNL team finalized the modification and design of the U-frame testing setup and the integration of the U-frame setup into a Bose dual linear motor test bench to develop a cyclic integrated reversible-bending fatigue tester (CIRFT).[4] A final check was conducted on the CIRFT test system in August 2013, and the CIRFT was installed in the hot cell in September 2013.

The fatigue responses of Zircaloy-4 (Zry-4) cladding, including understanding the role of pellet–pellet and pellet–clad interactions are critical to characterizing SNF vibration integrity, but such data are not available due to the unavailability of an effective testing system, as mentioned above. While the deployment of the CIRFT test system in a hot cell will provide the opportunity to generate the data, the use of surrogate rod during out of hot cell testing has proven quite effective in identifying the underlying deformation mechanism of a cladding and fuel composite rod under an equivalent loading condition. This paper presents the experimental results of using surrogate rods made of Zry-4 cladding and alumina pellets under reversible cyclic bend loading.

REVERSIBLE BENDING FATIGUE TEST SYSTEM

The reversible bending fatigue test system is composed of a U-frame for imposing the bending loads on the spent fuel rod test specimen as well as providing a method for measuring the curvature of the fuel rod during bending.[5] The U-frame setup consists of two rigid arms, linking members, and connections to a universal testing machine. A horizontal layout of the U-frame setup has been adopted to eliminate the effect of the components' weight on the bending of the rod specimen. The effect of component weights has been found to be substantial enough to cause the bending of the rod to deviate from the pure bending condition. Dual linear motors are used to apply the forces symmetrically at the two loading points. These linear motors use electromagnetic driving force and have been shown to be superior in hot-cell testing than other conventional actuation systems such as servo-hydraulic and electromechanical systems. In addition, it was demonstrated that the use of two linear motors can benefit symmetrical loading, especially during dynamic loading. The reciprocal motion of the two loading rod points when integrated into U-frame is converted into reversible bending of the rod specimen.

The current U-frame setup can accommodate a 152.40 mm (6 in.) rod specimen whose diameter can vary from 9.50 to 11.70 mm. The rod is coupled to the U-frame using two rigid sleeves that have an inside diameter (ID) of 15.00 mm, outside diameter (OD) of 25.00 mm, and length of 50.80 mm. The sleeves themselves are mounted to the specimen ends using cast epoxy. A gauge section of 50.80 mm (2 in.) is obtained once the specimen is installed to the U-frame.

The dual linear motors are mounted to a steel breadboard along with the U-frame setup. The system can deliver a load of ±3000 N and displacement of ±25.40 mm. The current setup is equipped with a 101.60 mm (4 in.) loading arm, so the maximum available moment of system for bending is ±304.80 N·m. The interface components assembled on the Bose dual linear motors test bench are shown in Fig. 1.

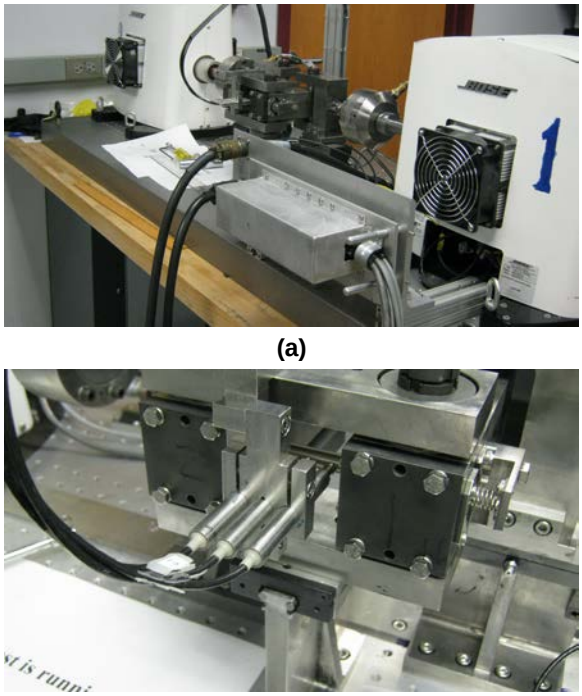

(a)

(b)

Fig. 1. (a) U-frame setup integrated to Bose dual LM2 TB, (b) the enlarged view of specimen section with three LVDTs mounted to simultaneously measure the deflections of the rod at three points.

PREPARATION OF ROD SPECIMEN

Two 5 ft Zry-4 tubes with OD 9.50 mm and ID 8.36 mm were sectioned into twenty 6 in. tubes. At the same time, ten 5/16 in. × 12 in. alumina rods were purchased. Each rod was then cut into 15.24 mm Rodlets. These small rodlets serve as pellets within the 6 in. Zry-4 cladding tube sections.

Pellet–cladding interaction was studied through simulations with and without epoxy bonding. Preparation of epoxy-bonded surrogate rods involved installing the alumina pellets while injecting epoxy on the internal surface of the cladding tubes and on the end faces of the pellets.

The mounting of the two rigid sleeves onto each rod specimen was accomplished using a vise mold. For the first rigid sleeve, mounting required injecting epoxy into the sleeve, transferring the sleeve to the loading chamber of the vise mold, inserting the rod, and closing the mold. For the second sleeve, only epoxy injection and transfer of the rigid sleeve were necessary. A 24 h curing period was generally needed to allow the epoxy to reach full strength. The detailed procedure is provided in Wang et al. (2013).[4] A commercial epoxy dual pack (DP420, 3M, St. Paul, MN) was used in this research. The studies demonstrated that the cast epoxy can serve as a compliant layer having the required durability in both cycle fatigue and hot-cell radiation environments. [1,4]

The specimens were designated as ZRAPxx (with “xx” indicating the sample number) for the surrogate rods made of Zry-4 cladding and alumina pellets with epoxy bonding, and as ZRAPMxx for those samples without epoxy bonding.

TEST PROCEDURE

1. Monotonic Testing

Monotonic testing was conducted under displacement control. The displacement channels of the test machine were set at a load rate of 0.2 mm/s to 10.00 mm and back to 0 mm at the same rate.

Such displacement control is equivalent to a unidirectional 0.01 Hz triangular wave. Because the dual linear motors and U-frame setup are connected in series, the applied displacement to the U-frame is accumulated. Thus, the total (or relative) maximum displacement in the test was 20.00 mm. As mentioned above, the bend of the rod was measured by using three linear variable differential transformers (LVDTs). Although the deflections themselves provided information related to a rod's deformation, it has been shown that these measurements involve an additional contribution from the compliant layer; therefore, the curvature was used in this study to characterize the bending of the rod. The test results are presented in terms of moment–curvature curves.

2. Cyclic Testing

The reversible cyclic bend testing consisted of (1) measurements at the specified number of cycles and (2) the cycling itself. The measurements included three cycles of 0.05 Hz sine waves with peak displacements of ±0.4, ±0.6, and ±0.8 mm. The cycling involved using 5 or 10 Hz sine waves under load control. The determination of the load amplitudes depended on the experimental results from monotonic testing. In general, the selected load amplitude captured lifetimes at 10^4, 10^5, and 10^6 cycles.

The cyclic test was stopped whenever the following events occurred: (1) the predetermined limits in displacement of motor1 or motor 2 exceeded 4 to 6 mm or (2) the accumulative cycle number exceeded 1 or 2 million. Data on displacements, loads, and LVDTs were collected during both the quasi-static measurements and dynamic cycling at defined sampling rate and intervals. The moment–curvature relationships were carefully examined and validated for each test. The curvature range, moment range, and flexural rigidity (moment per unit curvature)^1 were used in this study and are provided in this paper.

RESULTS OF MONOTONIC TESTING

The resistance of the U-frame to loading can be substantial, especially when the monotonic test demands a large displacement, with average readings of load channels as high as 40 N near the 10.00 mm displacement channels. Due to this issue, the load channel readings were corrected to take into account the resistance force from the system.

1. Surrogate Rod with Epoxy Bonding

Results for ZRAP01 and ZRAP02 are shown in Figs. 2 and 3. The loading results initially show a linear response, followed by a nonlinear stage with three unloading valleys before the peak point. These unloading valleys correspond to popping sounds emitted during the test. Optical microscopy of ZRAP01 revealed that multiple transverse cracks had developed; therefore, the unloading points observed on the loading curve for ZRAP01 may be related to cracking events. In the case of ZRAP02, however, no crack can be seen on the rod's surface, so it remains unclear whether the multiple unloading valleys correspond to cracks inside or outside the cladding tube. Detailed examination of the moment–curvature plot for each test showed a transition stage existing between 10 and 20 N·m. The loading before 10 N·m and after 20 N·m corresponded to two linear stages. A rigidity of 27.8 to 32 N·m was obtained through linear regression analysis of the initial stage. This value is quite close to the theoretical prediction assuming 10% of the full alumina rod rigidity is used.

Although the microprocess that dictated the behavior of the rod in this test is unclear, it is believed that the yielding of cladding and debonding of epoxy played critical roles in accelerating the fatigue of the rod. Therefore, the range of 10 to 20 N·m, or 100 to 200 N at the loading points of the U-frame, was set as the target amplitude range for the cyclic test discussed below. Later the upper bound of the load range was extended to 300 N to expand the range of the lifetime of the rod.

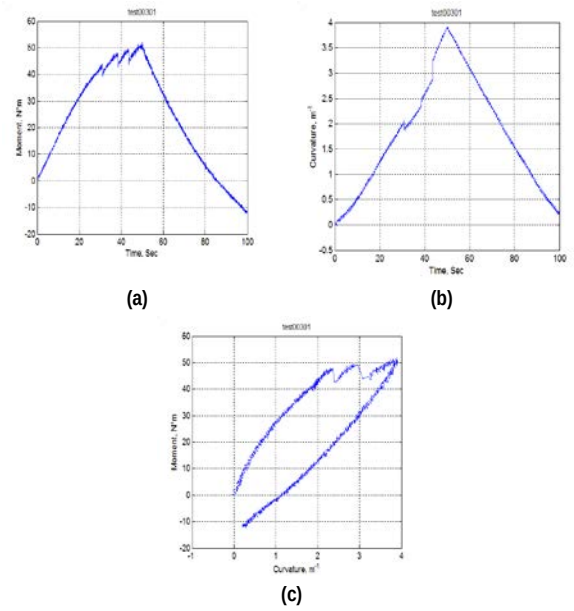

Fig. 2. (a) Moment, (b) curvature, and (c) moment–curvature curve for static bending test of ZRAP01 under 0.2 mm/s and maximum relative displacement of 20 mm at loading points of U-frame setup.

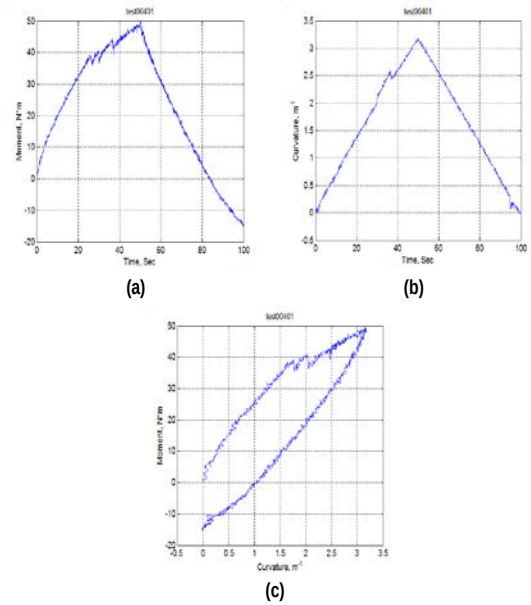

Fig. 3. (a) Moment, (b) curvature, and (c) moment–curvature curve for static bending test of ZRAP02 under 0.2 mm/s and maximum relative displacement of 20 mm at loading points of U-frame setup.

2. Surrogate Rod without Epoxy Bonding

The results for the rod specimen without an epoxy bond, ZRAPM01, are given in Fig. 4. It is interesting to see that both the maximum curvature and moment obtained under the same relative displacement of 20.00 mm are lower than those of ZRAP01. In particular, the maximum moment decreased from 50 N·m to 35 N·m. The estimate of flexural rigidity based on the initial linear stage of moment curvature resulted in a value of 14.5 N·m. This level of rigidity matches the theoretical prediction only if the contribution of alumina pellets is omitted; therefore, the impact of the epoxy bond on the response of the rod under bending is substantial. At the same time, the range of load amplitudes used in the cycle tests was the same as that for rods with an epoxy bond.

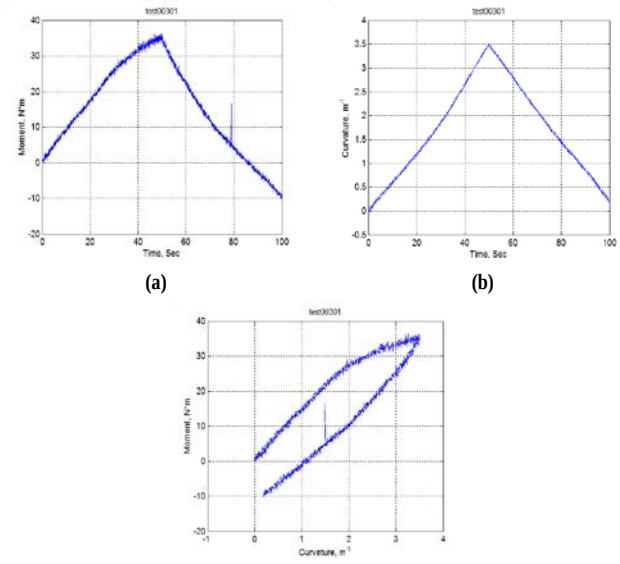

Fig. 4. (a) Moment, (b) curvature, and (c) moment–curvature curve for static bending test of ZRAPM01 under 0.2 mm/s and maximum displacement of 20 mm at loading points of U-frame setup.

RESULTS OF CYCLIC TESTING

1. Summary

A summary of the results for the cyclic tests conducted in this project along with the monotonic tests and calibration is provided in Table 1. The relationship of the moment to the number of cycles is given in Fig. 5. For the epoxy-bonded case, rod fractures were observed in most of the cyclic tests with moments greater than 10 N·m. Conversely, fractures were observed for the no-epoxy-bonding case at all moment levels.

The following sections discuss the fatigue test results for the surrogate rods, particularly in terms of flexural rigidity. This quantity can be monitored online, making it quite promising for characterizing the fatigue response of the reversible bending of rods.

Table 1. Summary of Zry-4 Surrogate Rod Tests

Specimen No.	Epoxy	Mode	Control	Amp.* (mm, N)	Amp. (mm, N·m)	Freq. (Hz)	Lifetime (N or N_f)	Notes
ZRAP01	Bond	Monotonic	Displacement	20	20	0.01		
ZRAP02	Bond	Cyclic	Load	100	10.16	5	1.27E+06	No failure
ZRAP03	Bond	Cyclic	Load	200	20.32	5	4.06E+04	Fractured
ZRAP04	Bond	Cyclic	Load	150	15.24	5	5.49E+05	Fractured
ZRAP05	Bond	Calibration	Load	80	8.128	1, 5,10		
ZRAP06	Bond	Cyclic	Load	200	20.32	10	7.25E+03	Fractured
ZRAP07	Bond	Cyclic	Load	200	20.32	10	6.38E+03	Fractured
ZRAP08	Bond	Cyclic	Load	100	10.16	10	2.00E+06	No failure
ZRAP09**	Bond	Cyclic	Load	150	15.24	5	2.22E+06	Fractured
ZRAP10	Bond	Cyclic	Load	175	17.78	5	5.86E+04	Fractured
ZRAP11	Bond	Cyclic	Load	200	20.32	5	4.17E+04	Fractured
ZRAP12	Bond	Cyclic	Displacement	10	10	0.01		
ZRAP13	Bond	Cyclic	Load	250	25.4	5	1.10E+04	Fractured
ZRAP14	Bond	Cyclic	Load	300	30.48	5	3.32E+03	Fractured
ZRAPM01	None	Monotonic	Displacement	20	20	0.01		
ZRAPM02	None	Cyclic	Load	200	20.32	5	6.71E+03	Fractured
ZRAPM03	None	Cyclic	Disp	150	15.24	5	2.31E+04	Fractured
ZRAPM04	None	Cyclic	Disp	100	10.16	10	7.44E+03	Fractured

* For displacement, the amplitude means that a relative displacement at the two load points of the U-frame was used.
** The last 79,000 cycles used 10 Hz in the cycle test.

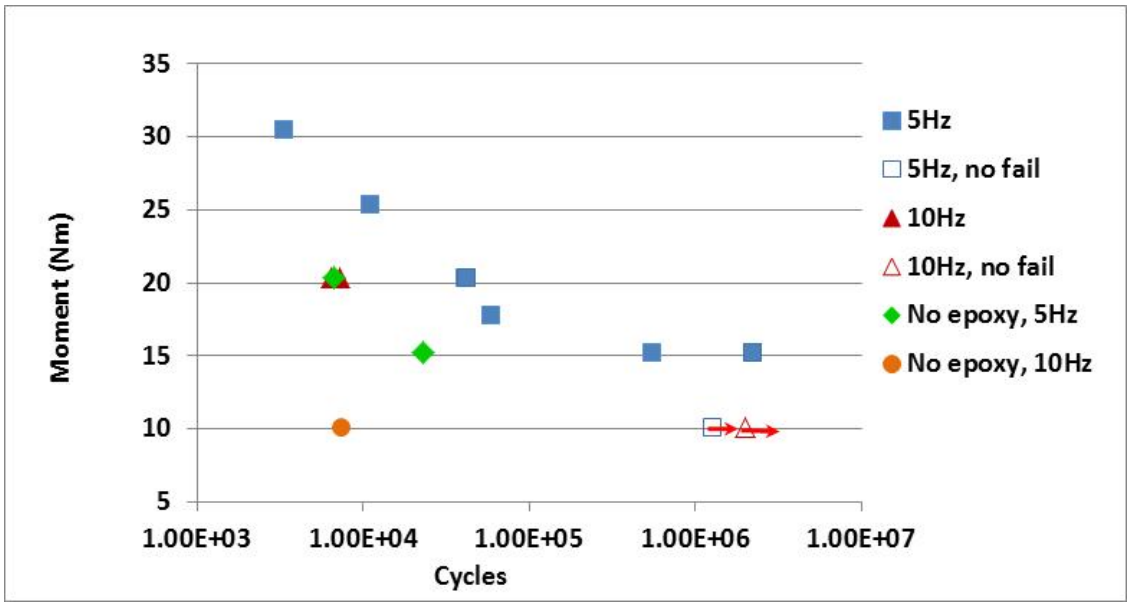

Fig. 5. Summary of cyclic tests of Zry-4 surrogate rods.

2. Surrogate Rod with Epoxy Bonding

The resistance of the system under dynamic loading or cyclic testing was found to be at the noise level, so the data processing of dynamic testing did not involve the data correction required for static loading because the level of loading amplitude is generally relatively small compared to that used in static loading.

2.1 Cyclic Testing at 5 Hz

Some results of the 5 Hz cyclic tests are presented in Figs. 6 to 10 for ZRAP02–ZRAP04, ZRAP10, and ZRAP13, respectively. Except for that of ZRAP02, all of the rigidity fatigue curves demonstrated a continuous decrease over the entire course of cyclic testing. The continuous degradation was also observed for ZRAP09, whose test (±150 N, 5 Hz) went beyond 2 million cycles. The specimen fractured shortly after the test was switched to 10 Hz to accelerate the fatigue. Another important observation is that for those fractured or cracked specimens, the degradation rate did not seem to change very much during cyclic testing, even when the specimen was about to fracture.

The results based on measurements exhibited variation comparable to those from online monitoring data. The selected curvature ranges for measurements allowed the bend of the rod to fall within the elastic region of the moment–curvature curve. These curvature ranges for measurements were all equal to or less than those used in cycling; therefore, the effect of measurement on the cycling is not believed to have been substantial, as validated by the concurrent changes of rigidity in both processes. For example, in the case of ZRAP02, the rigidity curves based on measurements were quite settled within a defined region, while that of online rigidity was stabilized near the 35 N·m² level. Figure 11 exhibits the fractured rods of specimens ZRAP03, ZRAP04, ZRAP09, ZRAP10, and ZRAP11. It can clearly be seen that all failures occurred in the gauge section.

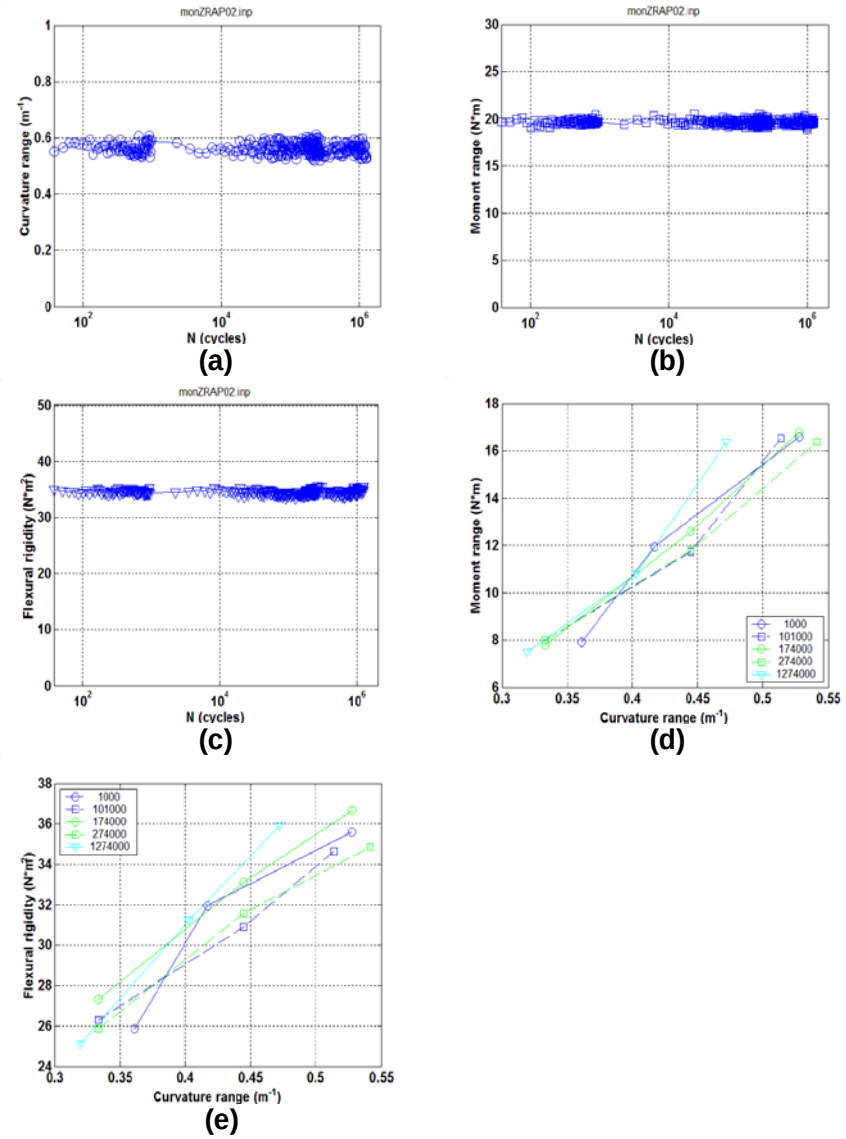

Fig. 6. Variation of (a) curvature, (b) moment, and (c) rigidity based on online monitoring; measurement results for (d) curves of moment versus curvature and (e) flexural rigidity versus curvature of ZRAP02: ±100 N, 5 Hz; no failure observed.

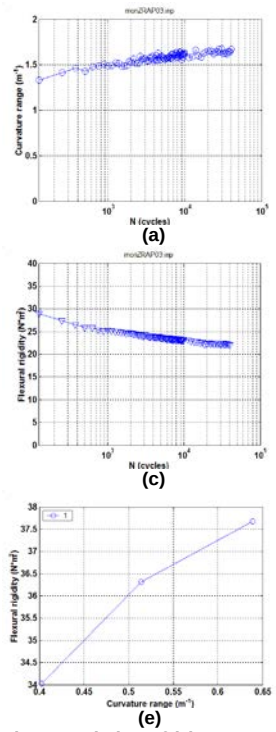

Fig. 7. Variation of (a) curvature, (b) moment, and (c) rigidity based on online monitoring; measurement results for (d) curves of moment versus curvature and (e) flexural rigidity versus curvature of ZRAP03: ±200 N, 5 Hz.

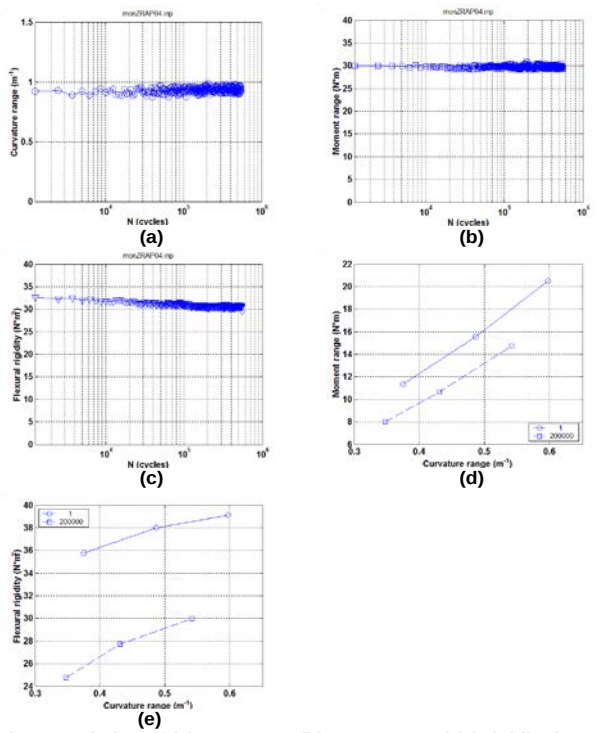

Fig. 8. Variation of (a) curvature, (b) moment, and (c) rigidity based on online monitoring; measurement results for (d) curves of moment versus curvature and (e) flexural rigidity versus curvature of ZRAP04: ±150 N, 5 Hz.

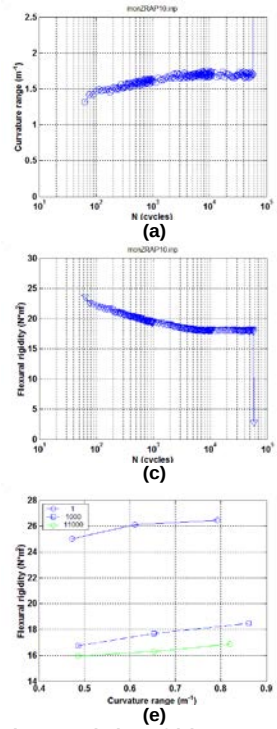

Fig. 9. Variation of (a) curvature, (b) moment, and (c) rigidity based on online monitoring; measurement results for (d) curves of moment versus curvature and (e) flexural rigidity versus curvature of ZRAP10: ±175 N, 5 Hz.

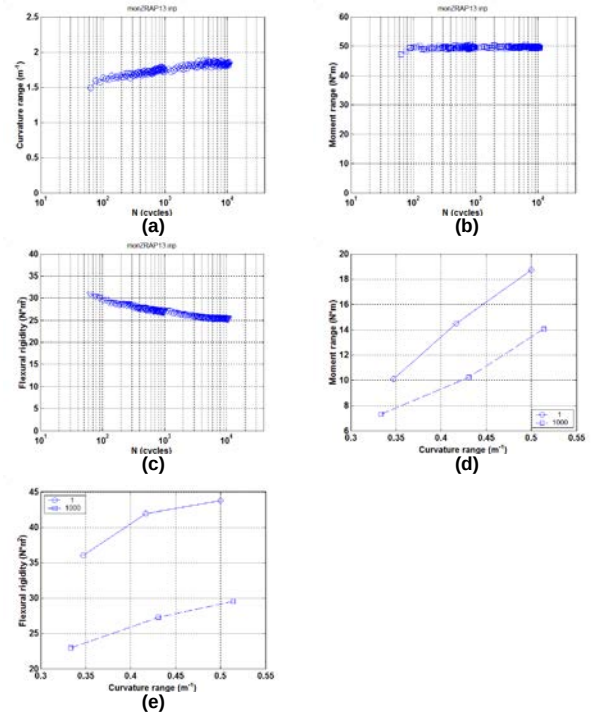

Fig. 10. Variation of (a) curvature, (b) moment, and (c) rigidity based on online monitoring; measurement results for (d) curves of moment versus curvature and (e) flexural rigidity versus curvature of ZRAP13: ±250 N, 5 Hz.

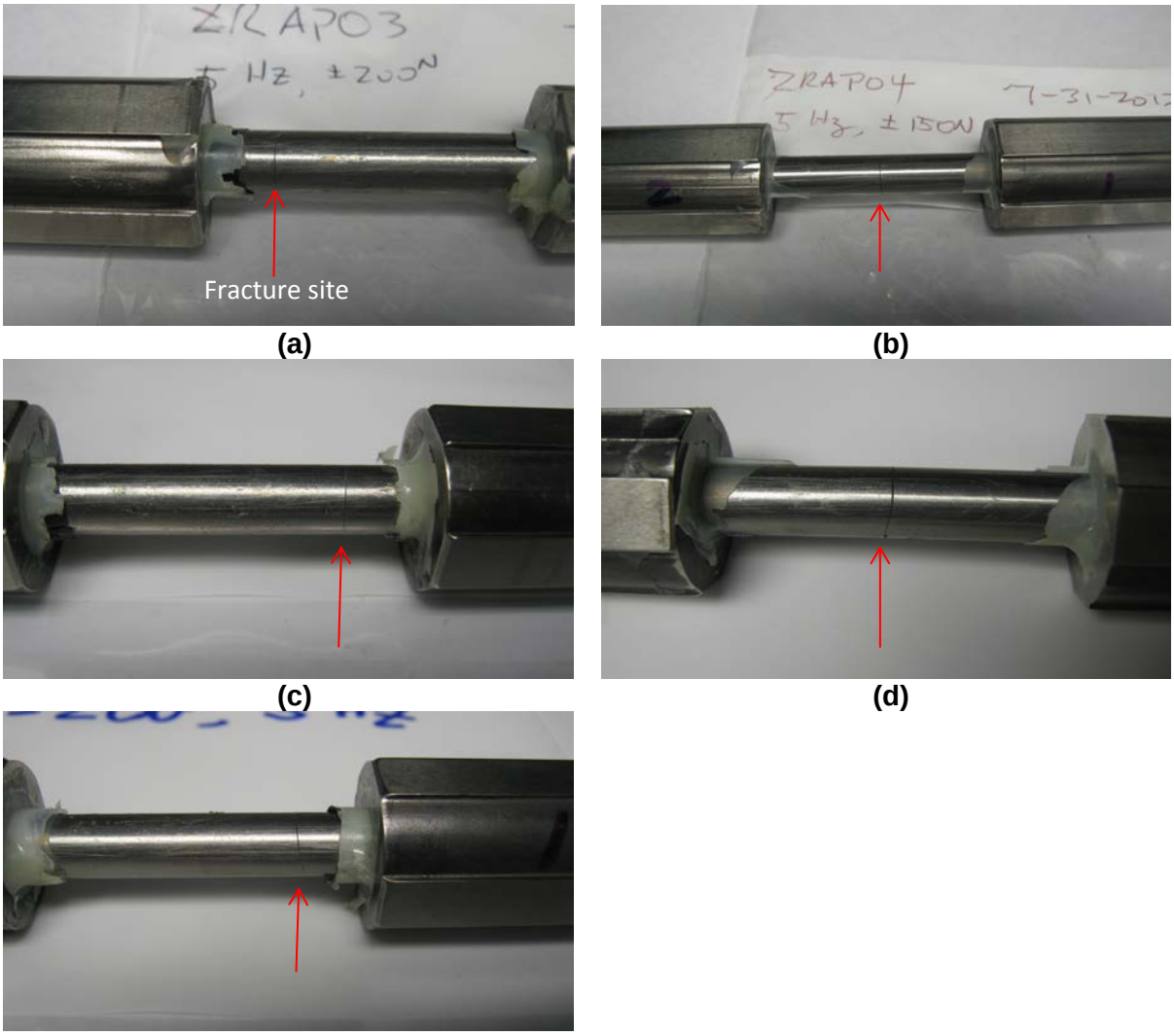

Fig. 11. Images showing fractured rods for (a) ZRAP03, (b) ZRAP04, (c) ZRAP09, (d) ZRAP10, and (e) ZRAP11. Red arrow indicates the fracture site.

3. Surrogate Rods without Epoxy Bonding

Cyclic testing on rods with no epoxy bonding was conducted at both 5 and 10 Hz. The 5 Hz tests were used for two high amplitudes, 150 and 200 N, and the 10 Hz test was used for low amplitude, 100 N. The use of 10 Hz in the 100 N cycle test represented an attempt to accelerate the fatigue test because that amplitude was expected to generate a long lifetime. As expected, the rods without an epoxy bond exhibited a relatively short lifetime compared to those of the epoxy-bonded rods. Under both 200 and 150 N, the rigidity continuously decreased prior to the fracturing of the rod specimen, as shown in Figs.12 and 13.

The test of ZRAPM04 under a low load revealed a surprisingly shorter lifetime (Fig. 14) than those under high loads. The rigidity based on online monitoring data was found to be near 7 N·m². Such low rigidity suggests that a structural flaw might be involved. Looking at the rigidity curve based on measurements, one can see that the flexural rigidity of this rod was still around 19 N·m² when the curvature range was near 0.5 m^{-1}. That level of rigidity is quite comparable to those of similar rods without epoxy bonding, as shown in Figs. 12 and 13. It is believed that ramping up of the load to the designed load level (100 N) during the 10 Hz cycle test clearly triggered the structural flaw, causing a marked increase in curvature, as shown in Fig. 14(a). The failure modes of the rods are illustrated in Fig. 15. All fractures are shown to have occurred within the gauge section.

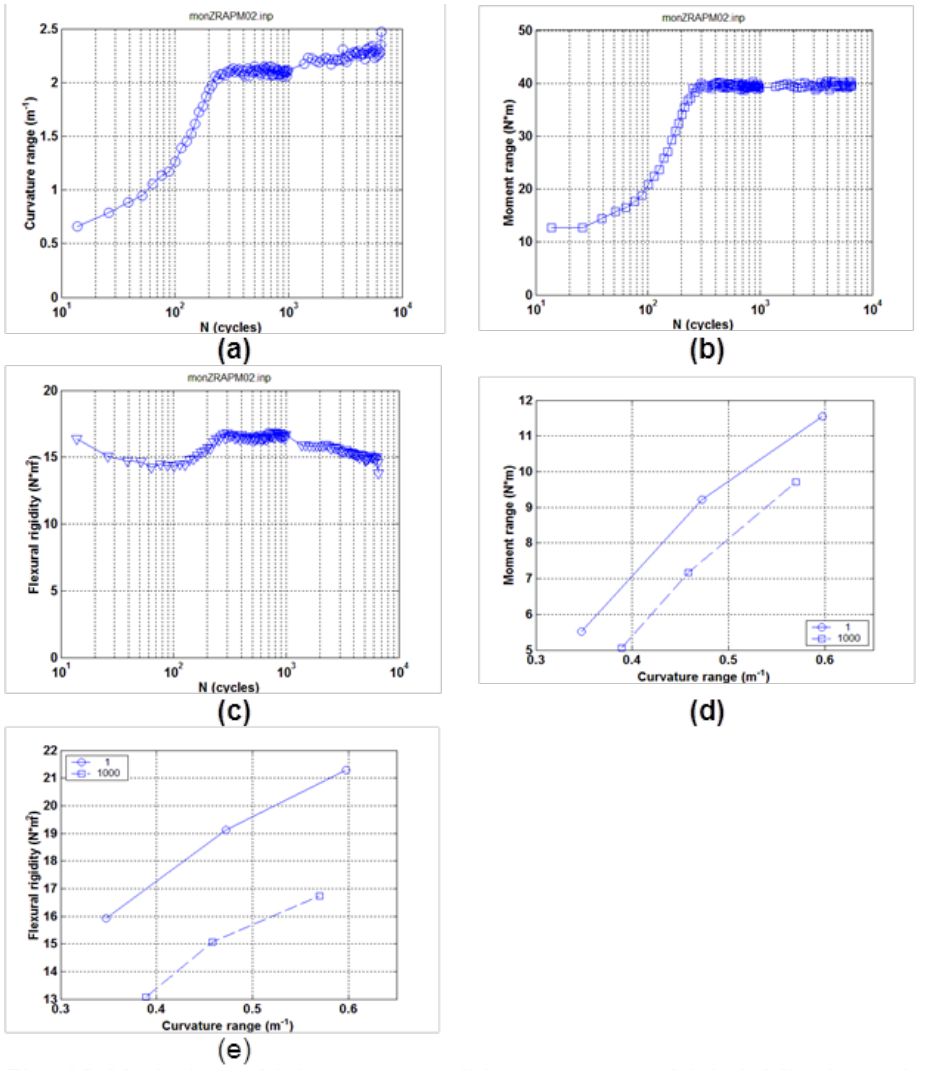

Fig. 12. Variation of (a) curvature, (b) moment, and (c) rigidity based on online monitoring; measurement results for (d) curves of moment versus curvature and (e) flexural rigidity versus curvature of ZRAPM02: ±200 N, 5 Hz.

DISCUSSION

1. Monotonic Testing

The monotonic test plays an important role in evaluating the vibration response of surrogate rods. Selection of appropriate amplitudes suitable for cyclic testing is critical for the monotonic bending test result of a rod specimen. The cyclic test results showed that within the target life of 10^4 to 10^6 cycles, several tests ran to several million cycles without rod failure. Therefore, the uncertainty related to the fabrication of a Zry-4 tube and preparation of a surrogate rod specimen could have a direct impact on the variability of test results. At least three to five specimens are

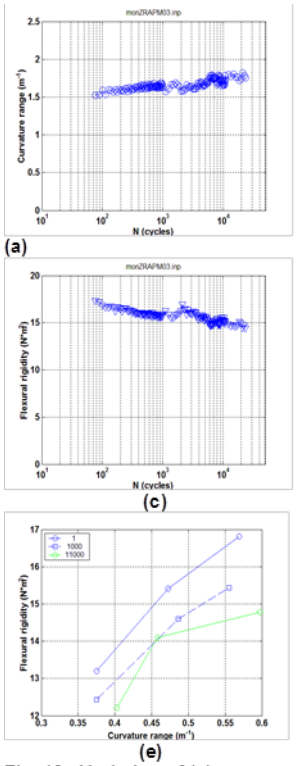

Fig. 13. Variation of (a) curvature, (b) moment, and (c) rigidity based on online monitoring; measurement results for (d) curves of moment versus curvature and (e) flexural rigidity versus curvature of ZRAPM03: ±150 N, 5 Hz.

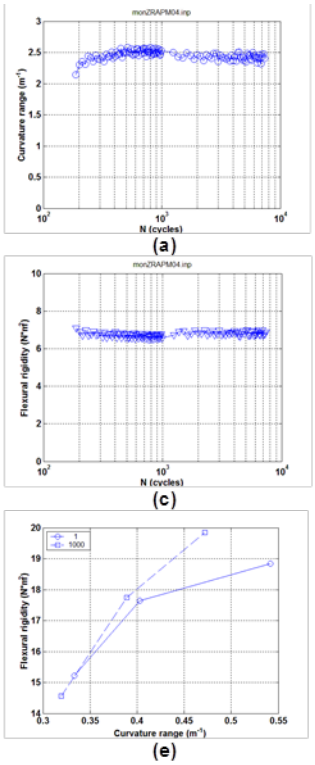

Fig. 14. Variation of (a) curvature, (b) moment, and (c) rigidity based on online monitoring; measurement results for (d) curves of moment versus curvature and (e) flexural rigidity versus curvature of ZRAPM04: ±100 N, 10 Hz.

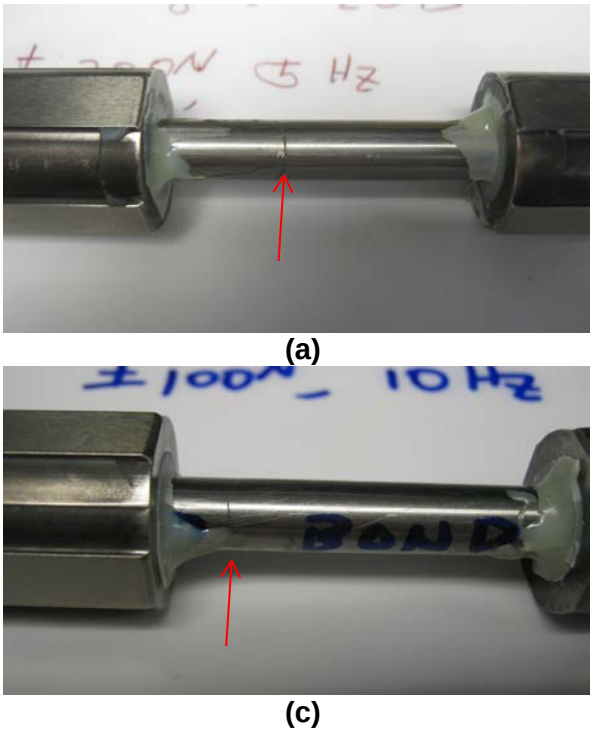

Fig. 15. Images showing fractured rods of (a) ZRAPM02, (b) ZRAPM03, (c) ZRAPM04.

needed to define the appropriate load amplitudes for cyclic testing. In a hot-cell fatigue strength evaluation, the effect of the above-mentioned uncertainties on the test's outcome could be more severe than that observed in the out-of-cell tests using surrogate rods because of the inherent multiscale discontinuities and complex residual stress profiles embedded in a high burnup SNF system.

In the fatigue strength evaluations, the maximum load amplitude was selected near the beginning of the nonlinearity observed in the monotonic moment-versus-curvature curve; the onset of the nonlinear regions is a result of clad yielding and other damage mechanisms associated with geometric nonlinearity within the composite rod. Currently the selections of target load level and load intervals for fatigue tests are largely based on trial and error. However, process uncertainty will be minimized when more control data are available.

2. Cyclic Testing

ORNL has also been developing a fatigue testing protocol using high frequency for hot-cell applications. This change is important because the protocol would significantly reduce hot-cell use, thereby lowering the overall cost of the project. However, there are constraints or limits on driving the system into higher-frequency applications from both the U-frame-setup and testing-machine perspectives. The frequency response of the Bose testing machine appears to be flat from 0 to 40 Hz, but the inherent dynamic property of the U-frame is the key that dictates the overall system frequency response in conjunction with the surrogate rod specimen.

By limiting the load level within the linear elastic range, we demonstrated that the measured curvature on ZRAP05 increased by specific degrees with 1 to 10 Hz increases in test frequency. An understanding of the controlled dynamic mechanisms of such accelerated aging will require further system investigation on a U-bend apparatus as well as development of more valid control data. Nevertheless, the dynamic factor should be considered when reconciling the lifetime differences between 5 and 10 Hz cycles, as shown in Fig. 6.

CONCLUSIONS

Monotonic and cyclic tests were conducted on surrogate rods made of a Zry-4-clad tube and alumina pellets, including samples with and without epoxy bonding. The conclusions drawn based on the test results and initial data analysis are as follows:

The flexural rigidity of the surrogate rod with epoxy bonding appeared to be much stronger than that of the rod without epoxy bonding for both monotonic and cyclic loading cases. Under the same loading amplitude, the surrogate rod without epoxy bond appears to have much shorter lifetime than that of rod with epoxy bond.

The surrogate rods with epoxy bonding fractured under cyclic bending for load amplitudes greater than 100 N, with a lifetime between 10^4 and 10^6 loading cycles. No failure was seen at the 100 N load level at up to 2 million loading cycles. An S-N curve is clearly defined for the cyclic test of epoxy-bonded rods.

The use of 10 Hz frequency in the cyclic testing apparently accelerated fatigue aging, which shortened the lifetime of the surrogate rod under a defined load level. A more detailed analysis is needed on the potential effects of dynamic inertia on the experimental results; this action item can provide further benchmarks for, and clarification to, the fatigue data obtained at higher-frequency bend loading conditions.

No defined S-N trend was obtained for the rods without epoxy bonding, which could be the result of uncertainties in the specimen machining condition, gap configuration at pellet–pellet and pellet–clad interfaces, and use of various testing conditions.

REFERENCES

1. J.-A. J. Wang et al., *High Burn-Up Spent Fuel Vibration Integrity Study Progress Letter Report (Out-of-Cell Fatigue Testing Development – Task 2.1)*, ORNL/ TM-2010/288, Oak Ridge National Laboratory, Oak Ridge, TN, 2011.
2. J.-A. J. Wang et al., *Progress Letter Report on U-Frame Test Setup and Bending Fatigue Test for Vibration Integrity Study (Out-of-Cell Fatigue Testing Development – Task 2.2)*, ORNL/TM-2011/531, Oak Ridge National Laboratory, Oak Ridge, TN, 2012
3. J.-A. J. Wang et al., *Progress Letter Report on U-Frame Test Setup and Bending Fatigue Test for Vibration Integrity Study (Out-of-Cell Fatigue Testing Development – Task 2.3)*, ORNL/TM-2012/417, Oak Ridge National Laboratory, Oak Ridge, TN, 2012.
4. J.-A. J. Wang et al., *Progress Letter Report on Bending Fatigue Test System Development for Spent Nuclear Fuel Vibration Integrity Study (Out-of-Cell Fatigue Testing Development – Task 2.4)*, ORNL/TM- 2013/225, Oak Ridge National Laboratory, Oak Ridge, TN, 2013.
5. H. Wang et al., "Development of U-frame bending system for studying the vibration integrity of spent nuclear fuel," *Journal of Nuclear Materials* **440**, 201–213 (2013).

ACKNOWLEDGEMENTS

The research was sponsored by the Office of Nuclear Regulatory Research, US Nuclear Regulatory Commission, under DOE contract DE-AC05-00OR22725 with UT-Battelle, LLC. The authors would like to thank NRC program managers Michelle Flanagan for providing guidance and support.

The development of the CIRFT device was sponsored by the Office of Nuclear Regulatory Research, US Nuclear Regulatory Commission, under DOE contract DE-AC05-00OR22725 with UT-Battelle, LLC. The authors would like to thank NRC program managers Michelle Flanagan for providing guidance and support in the device development process. The testing of surrogate material was sponsored by DOE UFDC and was conducted at Oak Ridge National Laboratory under contract DE-AC05-00OR22725 with UT-Battelle, LLC. The authors would like to thank Program Managers Harold Adkins for providing guidance and support to this project.